

## STUDYING THE INFLUENCE OF THE IMPACT GAP VALUE ON THE AVERAGE TRANSLATIONAL SPEED OF THE WHEELED VIBRATION-DRIVEN ROBOT

**Vitaliy Korendiy <sup>1</sup>, Oleksandr Kachur <sup>1</sup>, Volodymyr Gurskyi <sup>1</sup> and Pavlo Krot <sup>2</sup>**

<sup>1</sup> Department of Robotics and Integrated Mechanical Engineering Technologies, Lviv Polytechnic National University, Ukraine

<sup>2</sup> Faculty of Geoengineering, Mining and Geology, Wrocław University of Science and Technology, Poland

The double-mass vibro-impact system of the wheeled robot is presented in Figure 1. The crank  $AB$  rotates around the hinge  $A$  at a constant angular velocity  $\omega$ . The connecting rod  $DC$  is joined with the crank  $AB$  and pushes (pulls) the slider  $C$ . The latter is connected with the spring of the stiffness  $k_1$  actuating the impact body of the mass  $m_2$ . The maximal relative displacement of the impact body is restricted by the impact plate and spring of the stiffness  $k_2$ . The robot's body of the mass  $m_1$  is assembled on the wheeled chassis. Using the overrunning (free-wheel) clutches, the unidirectional rotation of the wheels is provided. In order to study the robot locomotion, the inertial coordinate system  $xOy$  and the corresponding generalized coordinate  $x_1$  are applied. The relative motion of the impact mass along the robot's body is described by the coordinate  $x_2$ .

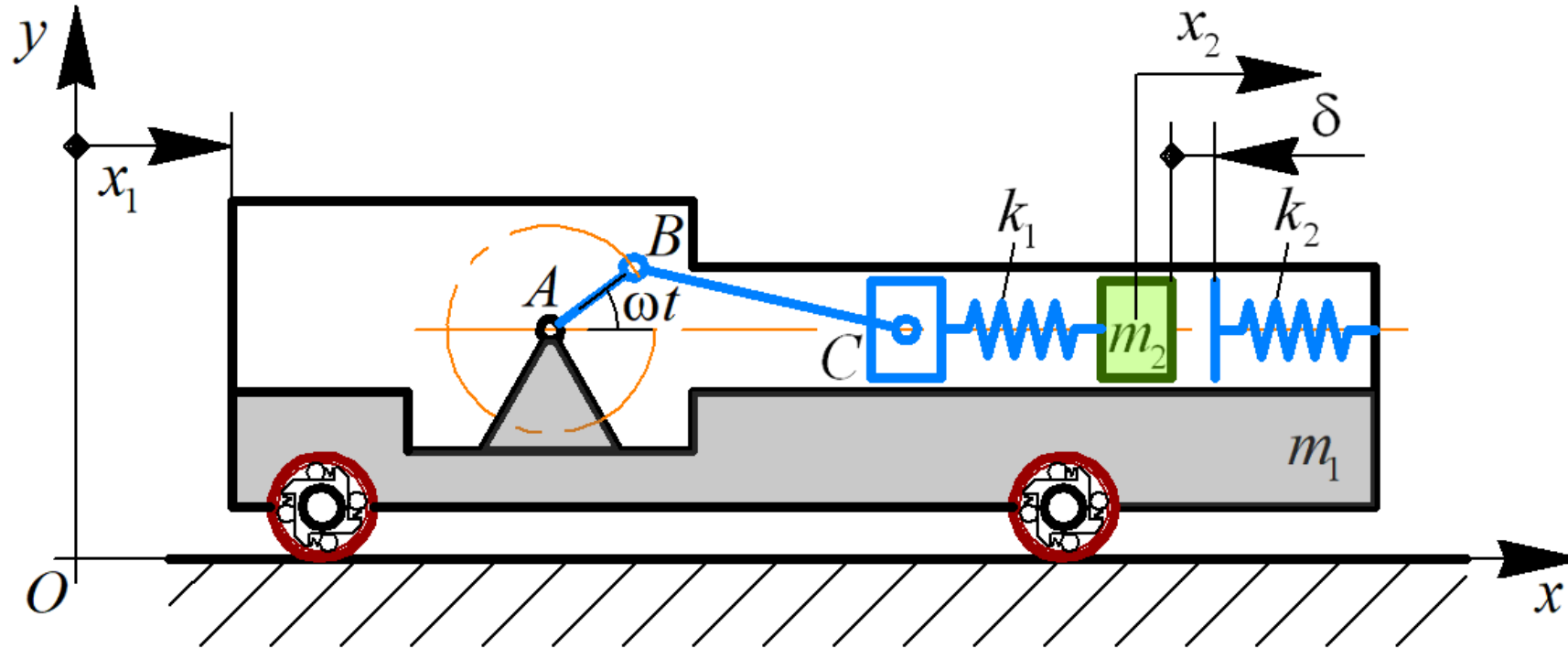


**Figure 1.** Simplified kinematic diagram of the wheeled vibro-impact robot.

Using the Euler–Lagrange equations, the simplified mathematical model describing the robot locomotion can be written as follows:

$$\begin{aligned}(m_1 + m_2)\ddot{x}_1 + (x_C - x_2)k_1 + (\delta_0 - x_2)k_2^* &= F_{br}, \\ m_2\ddot{x}_2 + (x_2 - x_C)k_1 + (x_2 - \delta_0)k_2^* &= 0,\end{aligned}$$

where

$$\begin{aligned}x_C &= l_{AB} \cos(\omega t) + \sqrt{l_{BC}^2 - (l_{AB} \sin(\omega t))^2} - l_{AB} - l_{BC} \underset{l_{BC} \gg l_{AB}}{\approx} l_{AB}(\cos(\omega t) - 1), \\ k_2^* &= \begin{cases} k_2, & x_2 \geq \delta_0, \\ 0, & x_2 < \delta_0, \end{cases} \\ F_{br} &= \begin{cases} 0, & \text{sign}(\dot{x}_1) \geq 0, \\ (x_C - x_2)k_1 + (\delta_0 - x_2)k_2^*, & \text{sign}(\dot{x}_1) < 0, \end{cases}\end{aligned}$$

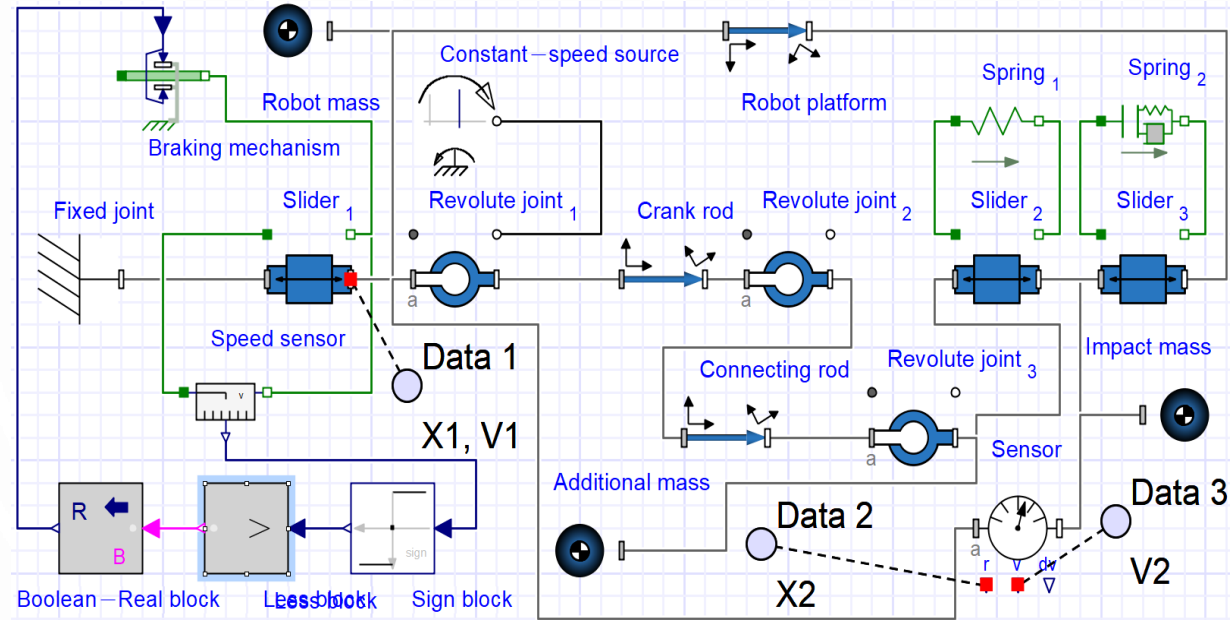
$l_{AB}$ ,  $l_{BC}$  are the lengths of the rods  $AB$ ,  $BC$ , respectively;  $\delta_0$  is the initial impact gap (the smallest distance between the impact mass  $m_2$  and the impact plate when the crank is in the state of rest and takes horizontal position).

The numerical modeling is carried out by solving the derived system of differential equations with the help of the Runge-Kutta methods in the Mathematica software.

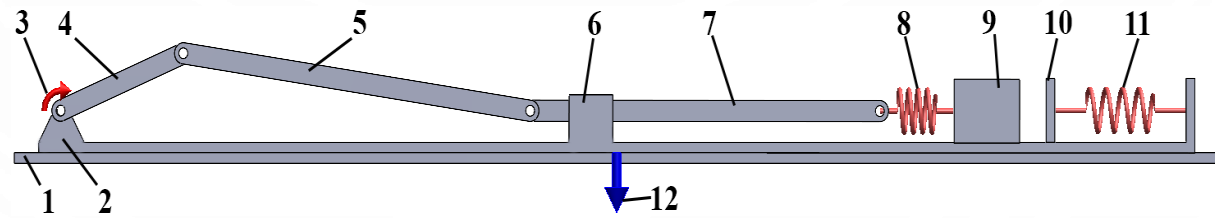
## Simulation models of the robot's oscillatory system

---

Along with the theoretical studies, the computer simulation of the robot's motion has been carried out. Figure 2 shows two simulation models of the robot's oscillatory system developed in the MapleSim and SolidWorks software. The models correspond to the robot's kinematic diagram considered above. The robot's body 2 is sliding along a horizontal surface 1. The rotary motor 3 actuates the crank 4 connected with the rod 5. The latter sets the sliding rod 7 into the rectilinear oscillatory motion along the guide 6. Due to the fact that the impact body 9 is connected with the sliding rod 7 by the spring 8, the oscillations of the body 9 are excited. The relative motion of the impact mass 9 is restricted by the impact plate 10 connected with the robot's body by the spring 11. In order to block the backward (leftward) motion of the robot's body, the special braking system 12 is used providing different values of friction forces for different motion directions.



(a)



(b)

**Figure 2.** Simulation models of the robot's oscillatory system: (a) MapleSim model; (b) SolidWorks model.

## Experimental prototype of the wheeled vibration-driven robot

---

To verify the results of the numerical modeling and computer simulation, the robot's experimental prototype has been designed and implemented in practice. The movable platform 1 is mounted on the wheeled chassis 2 (Figure 3). The overrunning (free-wheel) clutches 3 restrict the wheels backward rotation. The eccentric disc (crank) 4 is fixed on the motor's shaft 5. The control system 6 is based on the Arduino hardware and software. The rod 7 actuated by the eccentric 4 sets the sliding rod 8 into the oscillatory motion along the guide 9. The rod 8 is fixed to the upper end of the flat spring 10. Its lower end is connected with the impact body 11 sliding along the guides 12 with the help of the linear bearings 13. The motion of the impact body 11 is restricted by the rubber damper 14 fixed on the robot's platform. The motor 5 and the control system 6 are powered by the batteries placed in the boxes 17. The voltmeter-amperemeter 18 is used for registering the total power supply during the robot's motion under different operational conditions.

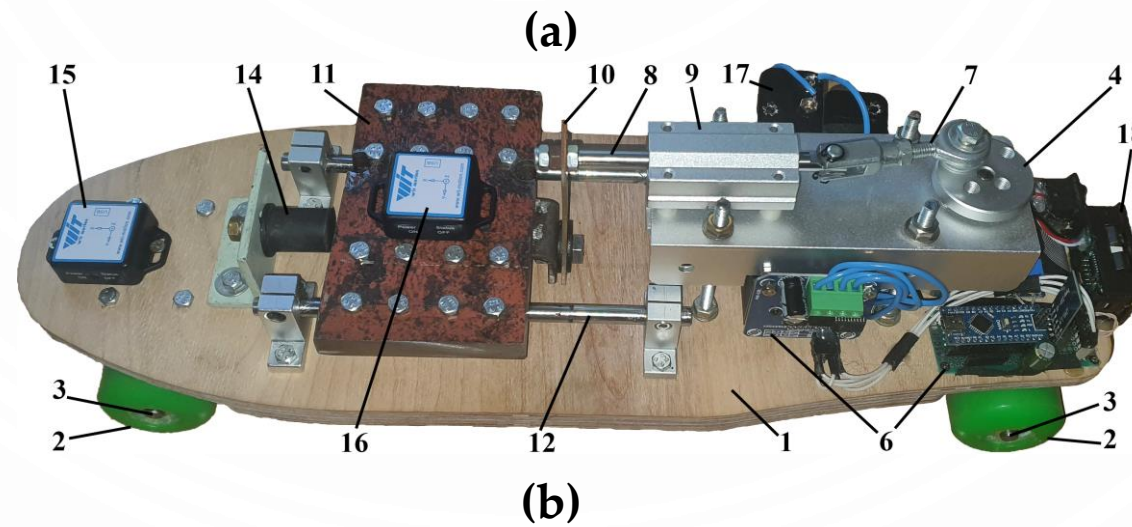
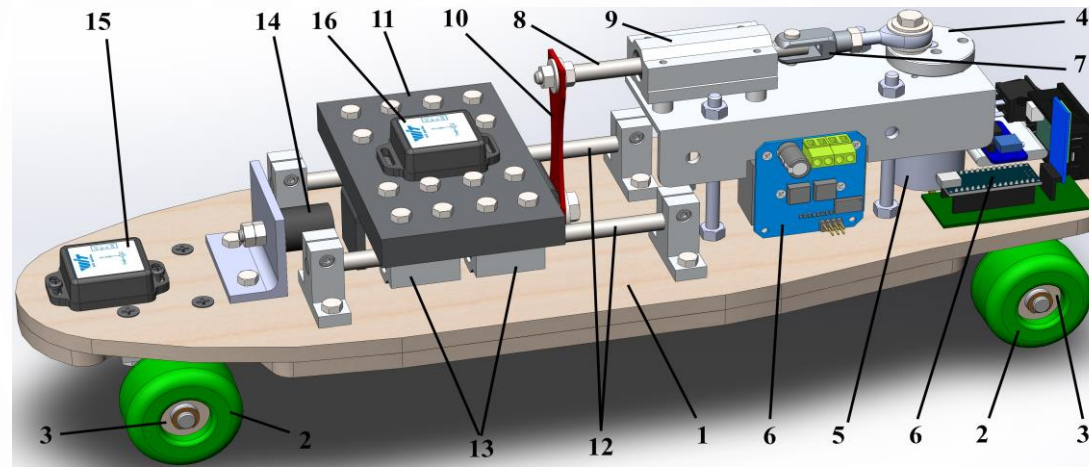


**Figure 3.** Experimental prototype of the wheeled vibration-driven robot:  
(a) 3D-design; (b) implemented robot.



## Results and Discussion

The study on the influence of the impact gap value on the average translational speed of the wheeled vibration-driven robot is carried under the following conditions. The robot moves along a horizontal rubber track; the power supply is constant; the inertial, stiffness and damping parameters of the robot's oscillatory system remain unchangeable. The only parameter being changed is the initial impact gap  $\delta_0$ , which can take the following values: 35 mm (nonimpact mode), 4 mm, 0 mm (impact modes) (see Figure 4).

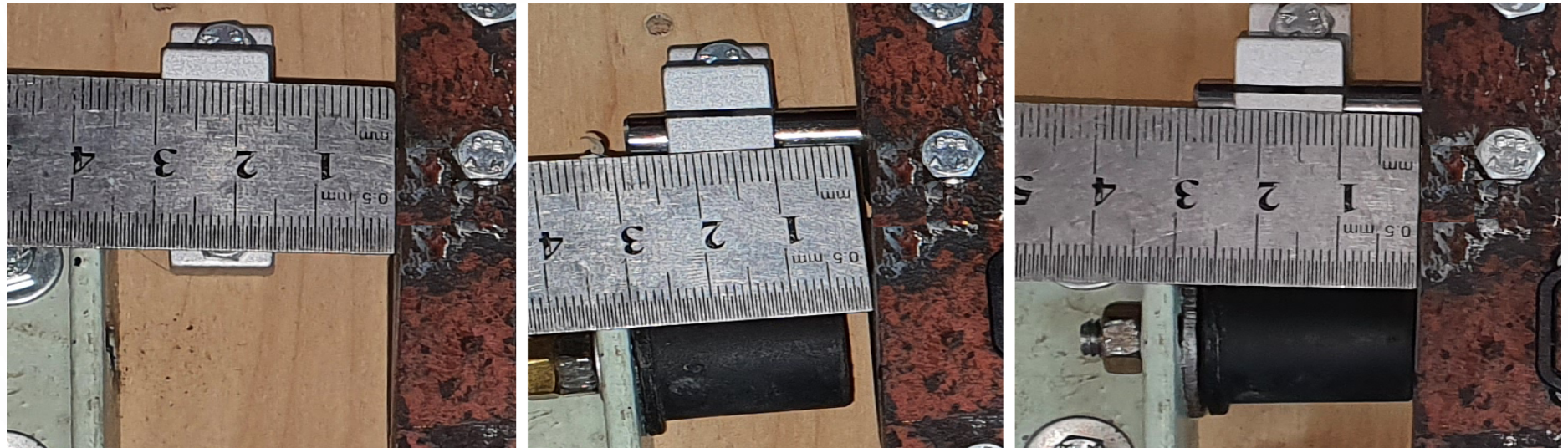


**Figure 4.** Three initial impact gap values being experimentally studied.

The numerical modeling has been carried out in the Mathematica software, while the computer simulation has been performed in the MapleSim and SolidWorks Motion software. Due to the fact that the obtained results are very similar, let us present only the plots obtained in the Mathematica software (see Figure 5) under the following input parameters:  $m_1 = 3.7$  kg,  $m_2 = 0.6$  kg,  $\omega = 37.7$  rad/s (6 Hz),  $l_{AB} = 0.025$  m,  $l_{BC} = 0.08$  m,  $k_1 = 800$  N/m,  $k_2 = 10^4$  N/m. During the time interval of 20 s (0...20 s), the robot's body passed the distance of 6.8 m at the initial impact gap of 4 mm; the distance of about 6.5 m – at the gaps of 2 and 6 mm; the distance of 5.9 m – at the gap of 8 mm. The smallest distance of 5.6 m has been passed under the zero-gap conditions. Therefore, the largest locomotion speed is about 0.34 m/s at the impact gap of 4 mm.

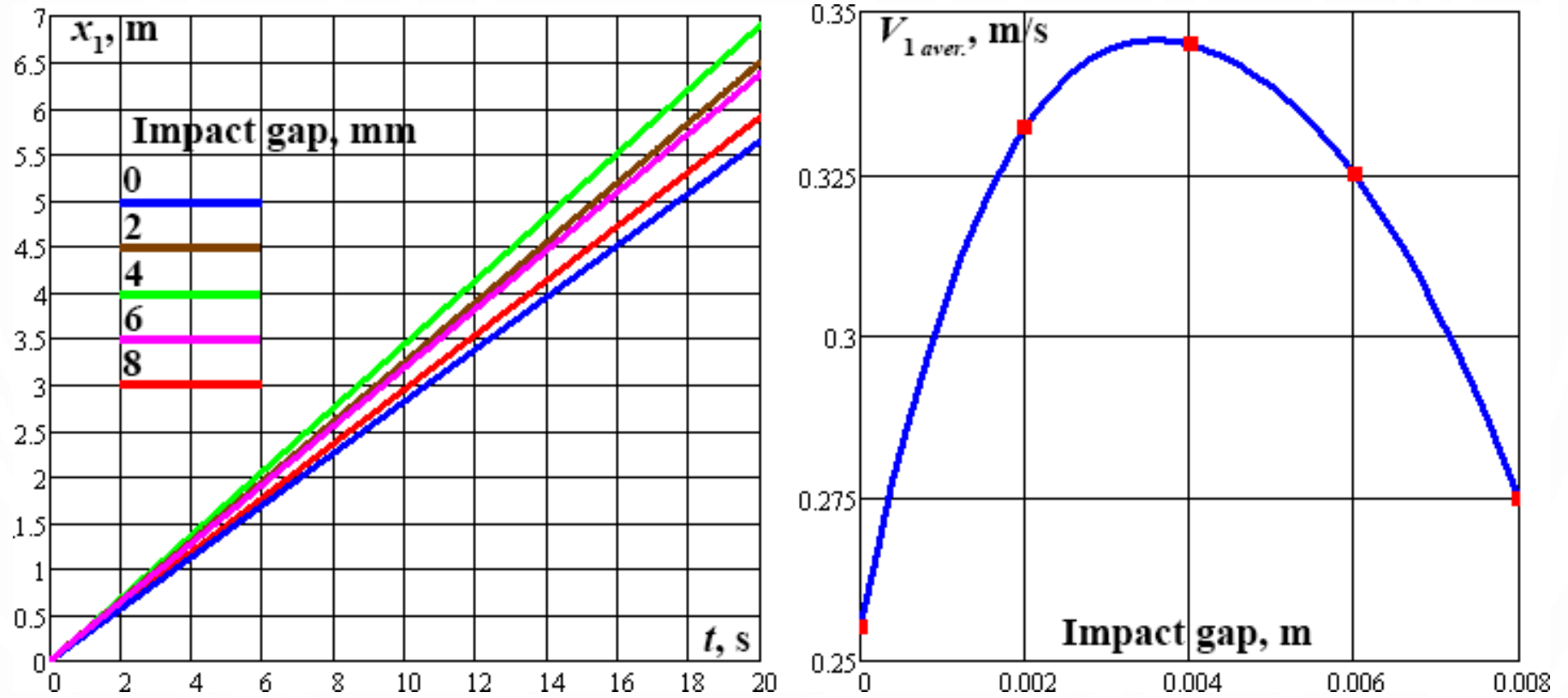


**Figure 5.** The numerical modeling results of the robot locomotion at different impact gap values.

## Experimental results

---

The experimental investigations (Figure 6) have been carried out at the Vibroengineering Laboratory of Lviv Polytechnic National University under three impact gap values: 35 mm (nonimpact mode), 4 mm, 0 mm (impact modes). The control system allows for providing the constant power supply to the robot's drive. In such a case, the forced frequencies took the following values 6.9 Hz (nonimpact mode), 6.3 Hz (impact gap of 4 mm), 5.4 Hz (zero-gap conditions). The wheeled platform and impact body accelerations have been registered by the WitMotion BWT901CL accelerometers. The experimental data have been processed with the help of the WitMotion and MathCad software.

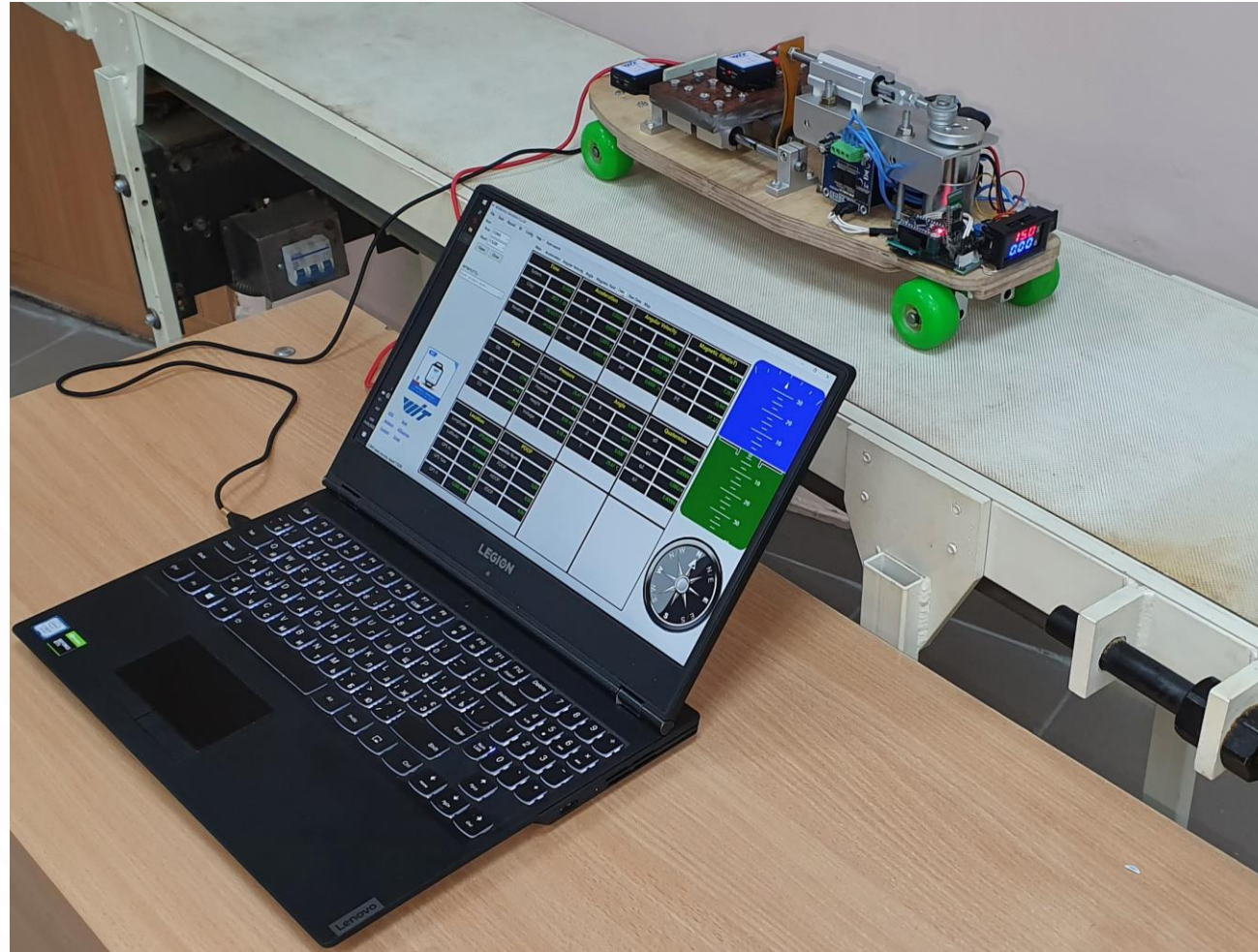


**Figure 6.** Experimental equipment used for studying the robot's locomotion conditions.

The results of experimental investigations are presented in Figure 7(a). The experimental data (curves 4, 5, 6) of the robot accelerations have been interpolated (curves 1, 2, 3) and numerically integrated with the help of the MathCad software. The corresponding time dependencies of the robot instantaneous speeds and displacements have been obtained (see Figure 7(b)-(c)). Numerical integration of the obtained results allows for concluding that the robot average locomotion speed reaches 0.34 m/s at the impact gap of 4 mm, whilst the use of the non-impact and zero-gap operational conditions provides almost equal average velocities of about 0.26 m/s. Some differences between the modeling results and experimental data can be explained by the fact that the forced frequency changes from 6.9 Hz under the non-impact conditions to 5.4 Hz at zero-gap mode despite the unchangeable power supply to the robot's drive.

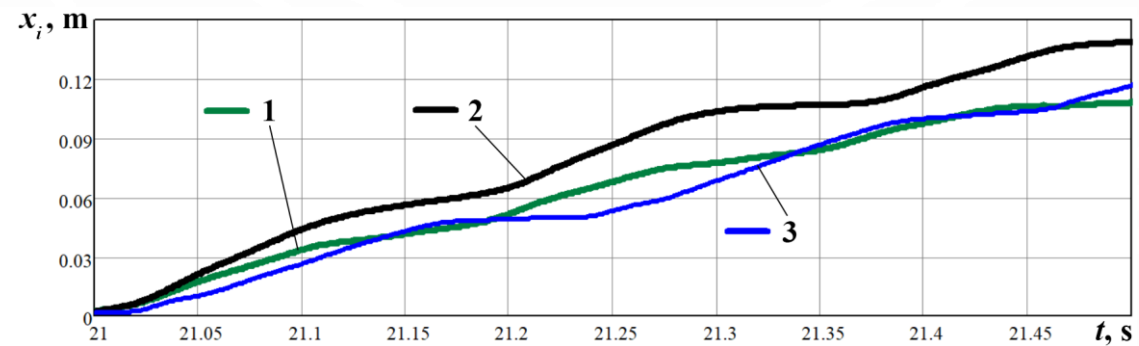
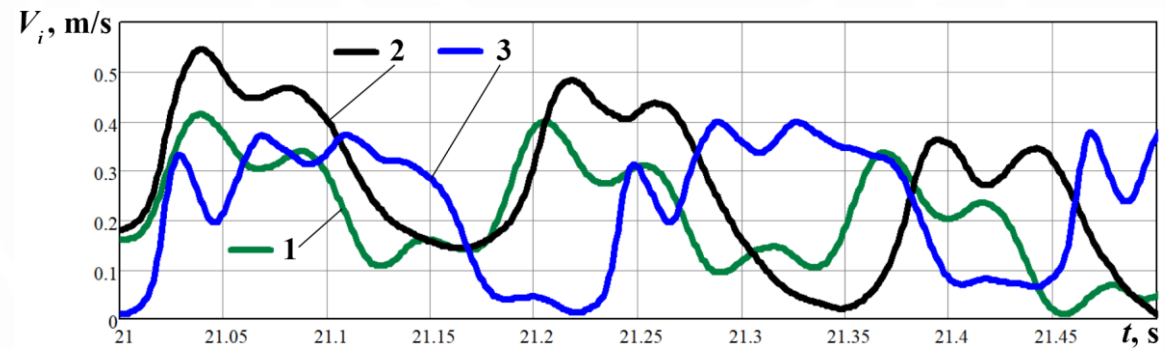
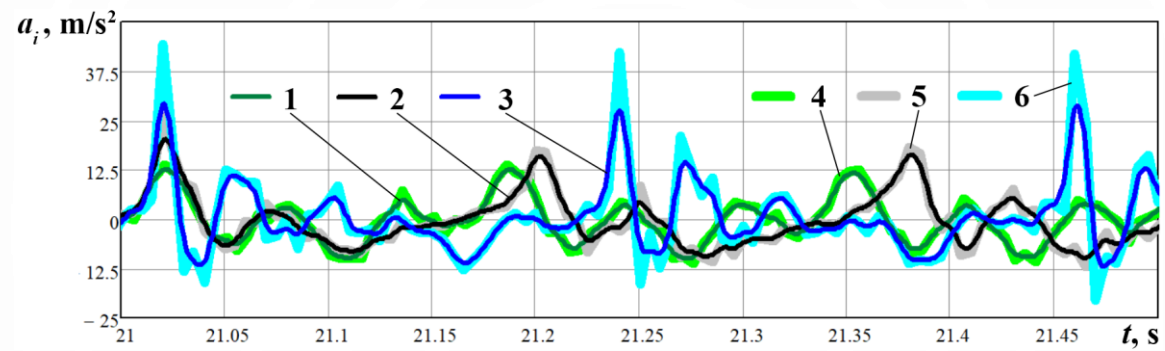


**Figure 7.** Experimental results of robot motion: (a) accelerations; (b) velocities; (c) displacements.

## Conclusions

---

The present paper is dedicated to studying the dynamic behavior of the wheeled vibration-driven robot. The robot's general design idea is proposed in the form of the 3D-model developed in the SolidWorks software and implemented in practice at the Vibroengineering Laboratory of Lviv Polytechnic National University. The mathematical model describing the robot locomotion is deduced using the Euler–Lagrange equations. The simplified computer simulation models of the robot's oscillatory system are developed in the MapleSim and SolidWorks software. The robot motion is numerically modeled, simulated and experimentally tested under different impact gap values. The obtained results satisfactorily agree with one another. Considering the forced frequency of about 5.4...6.9 Hz, the optimal impact gap value is in the range of 3...5 mm. In such a case, the robot's average locomotion velocity reaches 0.34 m/s. Herewith, the use of the non-impact and zero-gap operational conditions provides almost equal average velocities of about 0.26 m/s. The obtained results can be used by designers and researchers of similar robotic systems while choosing the optimal control strategies and defining the rational design parameters. The scopes of further investigations on the subject of the paper can be focused on analyzing the robot's drive power consumption under different operational conditions and studying the complex optimization parameter maximizing the robot's average locomotion speed and minimizing the drive power consumption.



**IECMA  
2022**

# **The 1st International Electronic Conference on Machines and Applications**

**15–30 SEPTEMBER 2022 | ONLINE**

**THANK YOU FOR YOUR ATTENTION  
AND LOOKING FORWARD TO  
COOPERATING WITH YOU!**